applied sciences

MDPI

Article

s-Guard: Multisensor Embedded Obstructive Sleep Apnea and Bruxism Real-Time Data Transmission Intraoral Appliance Device

Seo-Joon Lee [1], Il-Do Jeong [2], Eo-Bin Kim [2], Jin-Young Park [2], In-Hwan Jo [2], Jae-Hoon Han [3] and Tae-Young Jung [4,*]

1 Department of Medical Informatics, College of Medicine, The Catholic University of Korea, 222 Banpo Daero, Seoul 06591, Korea; richardlsj@naver.com
2 Department of ALFO Research Laboratory, Curaum Inc., Seoul 04307, Korea; ildojeong@curaum.com (I.-D.J.); eovinkim@curaum.com (E.-B.K.); pjy2437@curaum.com (J.-Y.P.); jojotan@curaum.com (I.-H.J.)
3 Department of Strategic Planning, Catholic University of Seoul, 222 Banpo Daero, Seoul 06591, Korea; jh.han531@gmail.com
4 Department of Research, VHS Education and Research Institute, Korea Veterans Health Service, Suwon 16275, Korea
* Correspondence: tyjung1983@gmail.com

Abstract: Obstructive sleep apnea (OSA) and bruxism are widely recognized as common forms of sleep obstruction in modern everyday life. The most representative and conventional treatment method using continuous positive airway pressure has a critical problem owing to its high inconvenience. A relatively modern alternative solution is the mandibular advancement device, but it still has no monitoring function for patient compliance. Therefore, this research proposes Sleep Guard (s-Guard), a multisensor embedded OSA monitoring intraoral appliance device based on Internet-of-Things technology. Relevant health information monitoring sensors, such as temperature, gyroscope, accelerometer, and SpO2 sensors, were embedded for real-time health monitoring. Results showed an average transmission speed of 91,870.19 bytes per second, a successful connection check rate of 100%, and a wireless data stream error rate of 0.1%. Overall, the actual speed, connection, and error test results revealed the robust functioning of s-Guard in real monitoring scenarios. This research is envisioned to greatly enhance patient compliance when treating OSA or bruxism and is also expected to motivate other sensors to be embedded in our proposed model for the application of other disease areas.

Keywords: OSA; bruxism; CPAP; MAD; sensor; IoT; intraoral appliance

Citation: Lee, S.-J.; Jeong, I.-D.; Kim, E.-B.; Park, J.-Y.; Jo, I.-H.; Han, J.-H.; Jung, T.-Y. s-Guard: Multisensor Embedded Obstructive Sleep Apnea and Bruxism Real-Time Data Transmission Intraoral Appliance Device. *Appl. Sci.* **2021**, *11*, 4182. https://doi.org/10.3390/app11094182

Academic Editor: In Young Choi

Received: 23 January 2021
Accepted: 22 April 2021
Published: 4 May 2021

1. Introduction

Considered the most common form of sleep obstruction, obstructive sleep apnea (OSA) is a life-threatening health anomaly that many people suffer from today. It is characterized by repeated pharyngeal airway collapse during sleep [1], which means that subjects' breathing frequently pauses while asleep, sometimes for minutes. Bruxism is another symptom that negatively affects sleep quality by significantly harming teeth and damaging temporomandibular joints (TMJ) [2].

Lack of sleep hinders focus and concentration during the day, causes chest pain upon waking up [3], causes morning headaches [4], and is a factor in many psychological symptoms such as depression, anxiety, or excessive irritability [5], and even death [6].

Continuous positive airway pressure (CPAP) treatment is the most commonly used method to treat OSA. It has proven to be the most effective way to prevent sleep obstruction because research has shown that subjects with OSA have significantly greater activity reductions in airway muscles than normal people [7,8]. A facemask is connected to a

machine via a tube and positive airway pressure is mechanically pushed directly into the mouth to keep the airways open (Figure 1).

Figure 1. CPAP device for treating OSA.

However, the problem with this universally accepted method is that it is simply too obstructive. In fact, an in-depth study concerning the effect of CPAP on sleep apnea syndrome revealed that patients showed discontent regarding CPAP because the device that was designed to enhance sleep quality paradoxically hindered sleep because it was too "bothersome" [9]. This naturally led to insufficient compliance rates; Yetkin et al. [10] proved that after months of compliance test results, only very severely affected patients adhered to CPAP devices until the end of the study period.

As a result, many alternative devices have been developed, such as the mandibular advancement device (MAD), which increases the airway diameter with soft tissue displacement achieved by mandibular protrusion [11]. It is a much smaller form of the oral device, compared to CPAP, which resembles the form of a mouthguard commonly used in sports (Figure 2). This oral device is also known to prevent bruxism in the absence of a CPAP device. A critical problem still persists with MAD in that there is still ongoing debate about the device's actual effectiveness in treating OSA. Many uncertainties regarding MAD have prevented comparably comfortable devices from becoming more widespread clinical sleep treatment services.

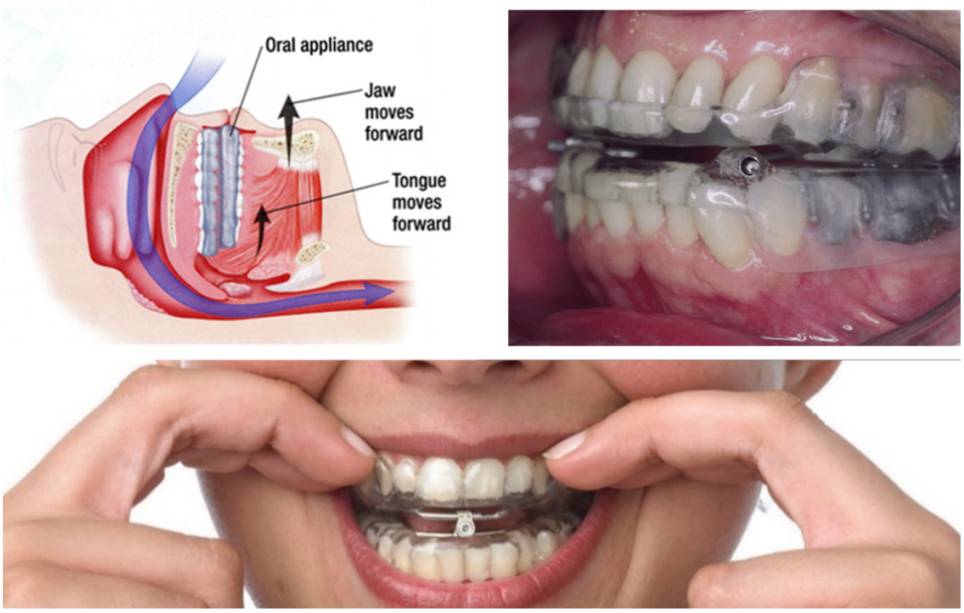

Figure 2. MAD [12] for treating OSA.

Therefore, this research proposes s-Guard: a multisensor embedded OSA monitoring intraoral appliance device specifically targeted for MAD prototypes. This research presents the unique design and development of the MAD-based model that enables sensors to be embedded and presents practical implementation results among institutional review board (IRB) approved subjects. Since this study targets OSA patients, relevant health information monitoring sensors such as temperature, gyroscope, accelerometer, and SpO_2 sensors were embedded. This research is expected to greatly motivate other sensors to be embedded in our proposed model for the application of other disease areas.

2. Related Literature

In the healthcare industry and business sectors, many innovations for global well-being are being developed as biosensor embedded solutions for enhancing health and wellness. The most commonly applied areas are wristband types, such as smartwatches [13] and ring types [14]. There are many other variations to monitor the health status of users/patients, but intraoral appliance-embedded healthcare solutions have rarely been addressed in previous research.

For example, Matsuda et al. demonstrated a sensor-embedded oral appliance to monitor the airway [1]. They fabricated maxillary and mandibular oral appliances from 2 mm thick resin plates using pressure welding. The activity of the left genioglossus (GG) was recorded using two silver ball electrodes attached to the lingual edge of the mandibular oral appliance. Respiratory status and right masseter muscle activity were measured using an airflow sensor and surface electrodes, respectively. Their attempts to apply sensors to oral appliances were impressive, although this solution was only designed for experimental purposes and not for practical purposes.

Jin et al. [15] developed a flexible surface acoustic wave respiration sensor for monitoring obstructive sleep apnea syndrome. They demonstrated the potential for flexible microsensors for monitoring OSA. Rocher et al. [16] also developed a smart system for monitoring apnea episodes in domestic environments with a sound sensor. Their proposed system consisted of a sound sensor, a vibrating element, and a microcontroller to process the collected data to detect OSA during sleep.

Some wearable-sensor-related researches targeted animal testing also. Zhang et al. [17] evaluated live mutton sheep during transportation based on a wearable multisensor system. More up-to-date literature review about the development of sensors are viewable from a review by Nasiri and Khosravani [18]. They systematically focused on applications of wearable sensors divided into (a) biophysical tracking, (b) biochemical monitoring, and (c) detection of real-time data.

Sekita et al. [19] developed a measuring system for 3D movement of the denture during function. The system for measuring denture movement consisted of an inertial measurement unit (IMU), a control unit, and a Bluetooth module. The IMU contained a three-axis gyroscope, a three-axis accelerometer, and a three-axis digital compass. The IMU was embedded in a self-curing acrylic resin. An important point of their research was that they successfully embedded several sensors despite the limited space allowed in dentures. They proposed a prototype that may serve as a future diagnostic appliance, such as occlusal examination in a denture, but this was also not developed to a practical level.

On the other hand, the current research proposes a multisensor embedded OSA monitoring intraoral appliance device, specially targeted for MAD prototypes. Compared to the recent research outlined above, our research was fully designed and tested for practical use. In addition, our proposed solution holds the highest number of embedded sensors known in all oral appliance-related studies thus far, which makes this research more unique considering the fact that MAD devices allow even less space tolerance, compared to normal dentures.

3. Overall System

3.1. Overall Service System Application

The overall system description of the proposed solution, s-Guard, is depicted in Figure 3. First, patients who use s-Guard need to be diagnosed with OSA after polysomnography (PSG) testing. Although s-Guard itself provides sleep quality monitoring functions, it is "treatment-centered" rather than "monitoring-" or "diagnosis-centered".

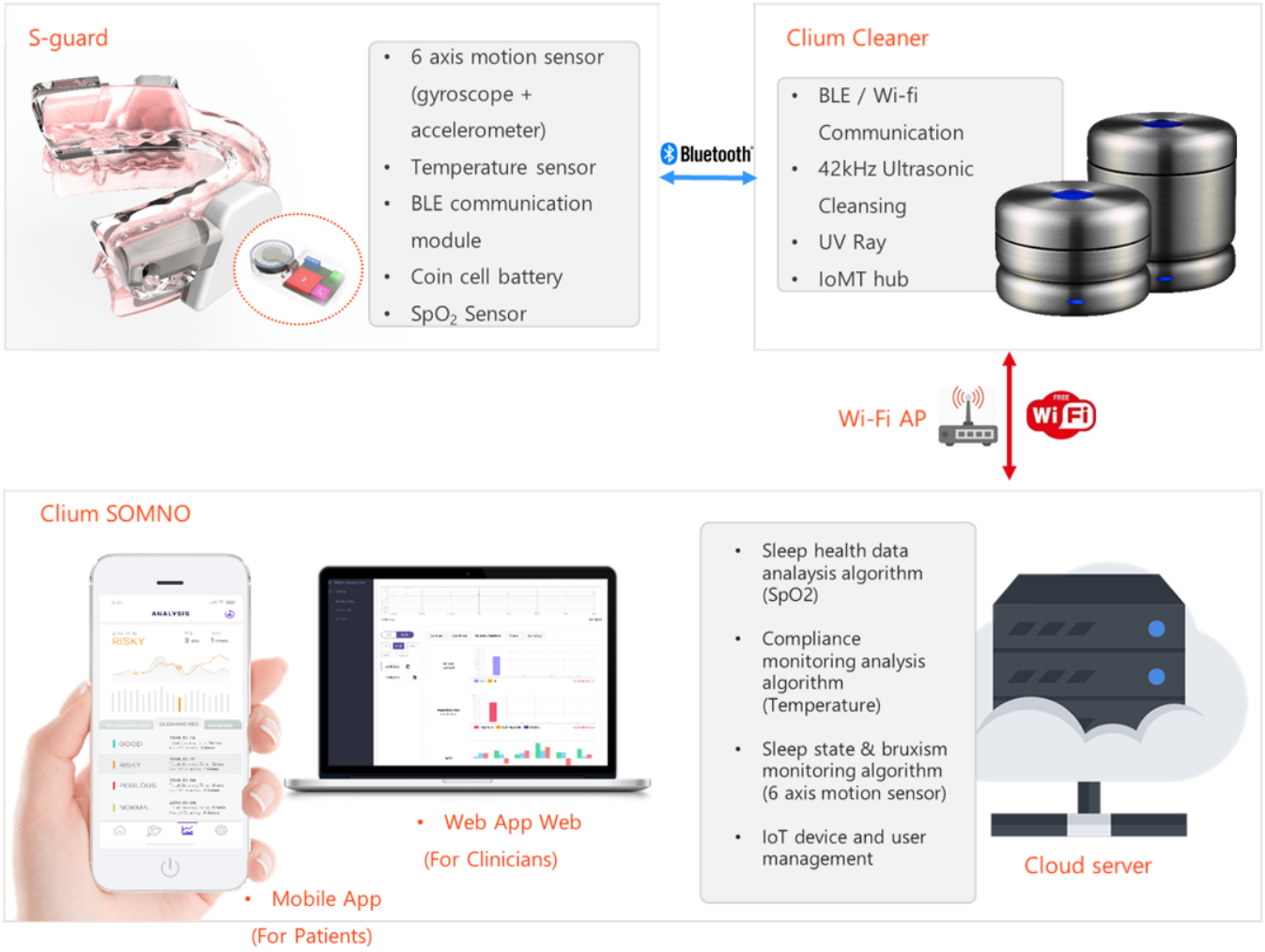

Figure 3. Overall system architecture.

In our proposed sensible intraoral appliance s-Guard, six-axis motion sensors (composed of a three-axis gyroscope and a two-axis accelerometer) [20] are embedded to monitor the sleep state and bruxism state. In addition, temperature sensors and SpO_2 sensors were embedded to monitor compliance status (measurement of properly complying to device usage) and OSA status, respectively. Finally, Bluetooth low energy (BLE) [21,22] communication module, microcontroller unit (MCU), and coin cell battery were used for the overall chip operation.

Healthcare data sensed from s-Guard are then transmitted to the MAD cleaner (named Clium) via Bluetooth communication. This is because the Bluetooth protocol is a form of near-field communication (NFC) [23], which basically needs a form of gateway to fully communicate with a server for full-service launch.

Raw data are then transmitted to the server from the cleaner communication hub through a Wi-Fi access point (AP). Other forms of fourth- (4G) or fifth-generation (5G) wireless communication can be applicable.

In the server, a sleep health data analysis algorithm is loaded to analyze the SpO_2 data. A compliance monitoring analysis algorithm was conducted based on temperature sensing data. The sleep state monitoring algorithm analyzes data obtained from six-axis motion sensors (accelerometer and gyroscope). The bruxism status can be additionally analyzed using this function. Servers also manage connected IoT devices and users. The specific design and development features of the sensible intraoral appliance, s-Guard, are explained in Section 3.2.

Statistical data analyzed from the server can be viewed by the patients through the mobile application. Only basic statistical data that could be easily perceived by no-professional patients are provided. More professional diagnosis-, treatment-, and monitoring-related data are provided to clinical professionals by the web application that is fully accessible through PC.

3.2. Specific Features of s-Guard

3.2.1. Design

A 3D design model prototype of the proposed sensible intraoral appliance s-Guard is shown in Figure 4. We used the capacity allowed in the inner cheek part of the MAD to embed sensory parts. The shape of the MAD is subordinate to the designated user. Figure 4a depicts the slide-on type of the sensory part, and Figure 4b depicts the screw-in type. A limitation of this model is that this design only supports patients/users older than 19 years old (adults only). This was due to the lack of capacity allowed when applied to younger ages with smaller inner oral sizes. In this paper, the slide-on type of s-Guard is shown.

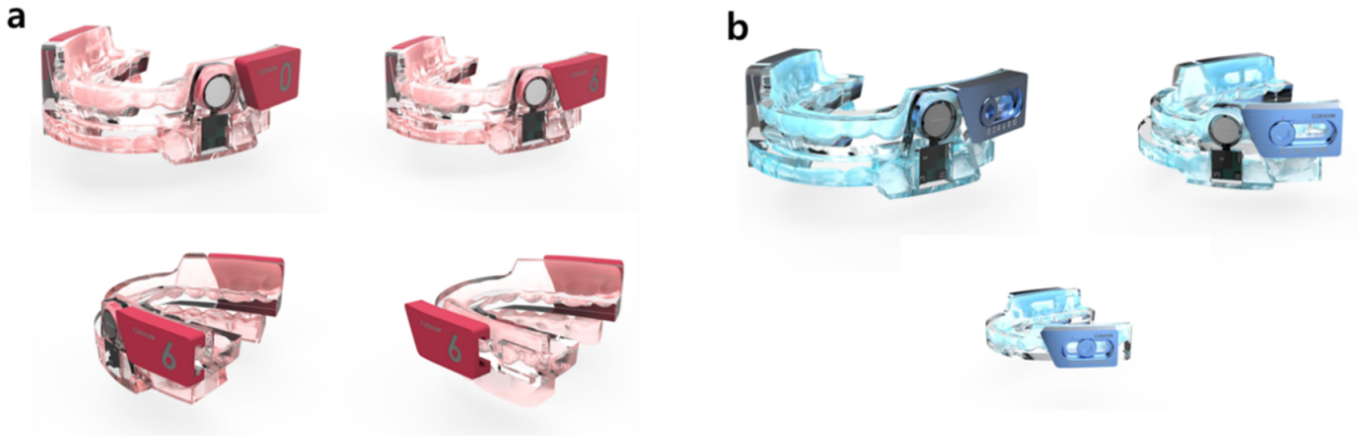

Figure 4. Cover-sliding type (**a**) and button-sliding type (**b**) 3D design concept model of s-Guard prototype.

Figure 5 shows the actual slide-on prototype model of the s-Guard. The MAD part was adjusted to fit the individual patient/user through a dental prescription. The lower jaw forward movement adjustment part provides the patient/user breathing space. All sensors and modules were embedded in the slide-on sensory parts. This part can be attached and detached to replace the power supply battery. SpO_2 is sensed through our solution by reflecting the data obtained from the vein and artery in the dermis part of the gums.

3.2.2. MCU, Communication Module, and Power Supply

The printed circuit board (PCB) and circuit schematic of s-Guard are shown in Figure 6. MCU, communication module, power, and other specifications are listed in Table 1. In summary, important features such as 64 Megahertz (MHz) 32-bit Advanced RISC Machine (ARM) Cortex-M4 was used for MCU, Bluetooth 5/Antenna (ANT)/2.4 Gigahertz (GHz) proprietary was used for communication module, and voltage (V) supply of 1.7 to 3.6 V low dropout (LDO) or direct current/direct current (DC/DC) was used for power.

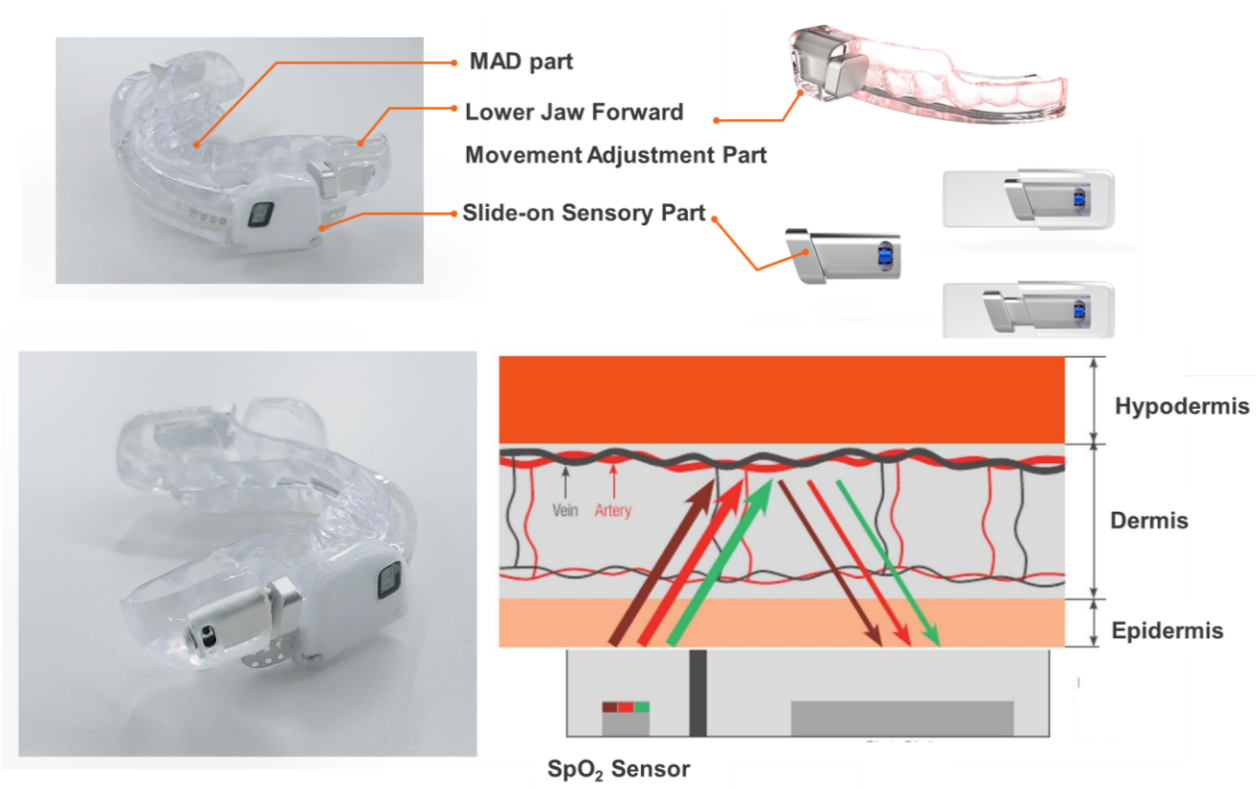

Figure 5. Actually manufactured slide-on prototype model of s-Guard.

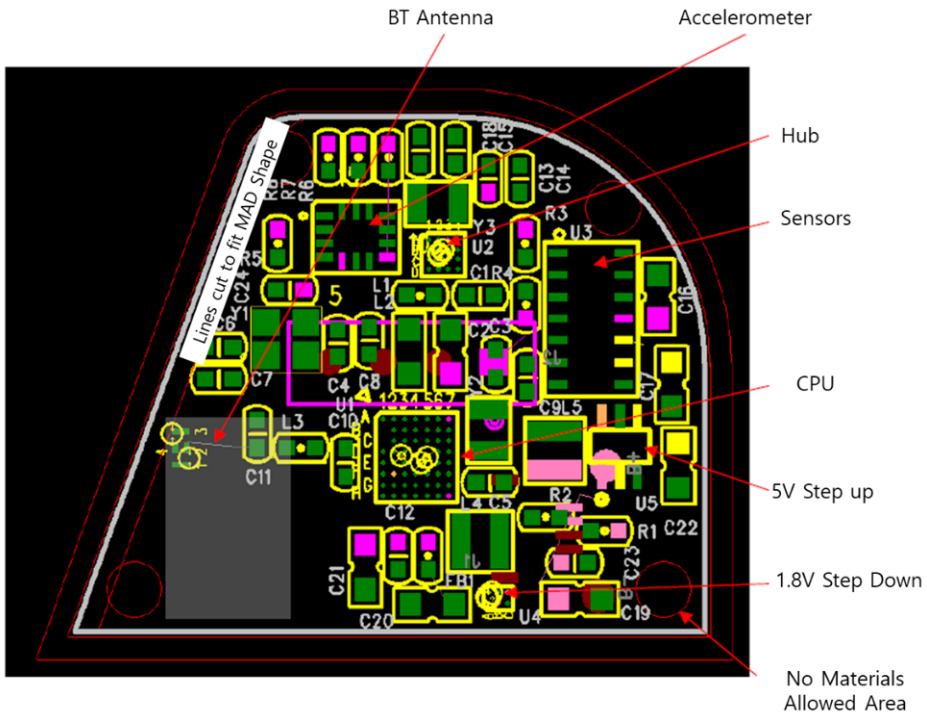

Figure 6. PCB and circuit schematic of proposed s-Guard.

Table 1. Core specifications of MCU, communication module, power supply, etc.

Classification	Specifics
MCU	64 MHz 32-bit ARM Cortex-M4
Communication Module	Bluetooth 5/ANT/2.4 GHz proprietary
Power supply	1.7 to 3.6 V LDO or DC/DC
Memory	192 KB Flash + 24 KB RAM
On-air data rate	2 Mbps/1 Mbps
TX power	Programmable from +4 to −20 dBm in 4 dB steps
Sensitivity	Bluetooth 5: 93 dBm at 2 Mbps
Radio current consumption DC/DC at 3 V	7.0 mA at +4 dBm TX power
System current consumption DC/DC at 3 V	0.3 µA in System OFF, no RAM retention, 0.5 µA in System OFF, full RAM retention
Hardware security	128-bit AES CCM, ECB, AAR
Digital interfaces	SPI master/slave, TWI master/slave, UART, PWM, QDEC, PDM
Analog interfaces	12-bit 200 ksps ADC, RNG, GP comparator
Peripherals	3 × 32-bit Timer
Package options	6 × 6 QFN48 [24] with 32 GPIOs, 5 × 5 QFN32 [25] with 16 GPIOs

3.2.3. Sensors

Core embedded sensors related to temperature, six-axis, and SpO_2 are presented in Table 2. On the board, SpO_2 includes algorithms, quick evaluation and data collection, stream data to mobile apps, schematics, or Gerbers to download, with components of MAX30101 (Optical Module) and MAX32664A (Algorithm MCU). The sampling rate per second (SPS) for the temperature sensor, six-axis sensor, and SpO_2 sensors were 2 SPS, 10 SPS, and 10 SPS, respectively.

Table 2. Specifications of temperature, six-axis, and SpO_2 sensors.

Classification	Specifics
Temperature Sensor	MAX30101 [26], −40 Celsius to +85 Celsius operating temperature range
six-axis Sensor	LSM6DSOX [27], iNEMO inertial module: always-on three dimension (3D) accelerometer and 3D gyroscope
SpO_2 Oscillators	64 MHz from 32 MHz external crystal or internal, 32 kHz from crystal [28], RC or synthesized

4. Results

4.1. Communication Speed Evaluation

The most important features of s-Guard include stable sensors, wireless communication, and seamless monitoring. Necessarily, this can be assessed mainly by two categories: communication speed and communication errors. This section presents the Bluetooth communication speed function evaluation results. The results will be followed by communication error rate performances that represent the stability of the fast communication in the next Section 4.2. The communication experiment was conducted using the experimental model shown in Figure 7. s-Guard was connected to our custom-developed MAD cleaner communication gateway (Clium) via Bluetooth. This gateway acts as a communication hub for server/personal computer (PC) connections and can also be used as a sanitized intraoral device storage.

Figure 7. Experiment model of s-Guard Bluetooth communication performance.

The MAD cleaner communication gateway was then connected to the test PC via a serial connection. Bluetooth communication speed performance was shown in a basic disk operating system (DOS) interface, which was shown in the console command in bits per second (bps). The specifications of the mad cleaner communication gateway and test PC are listed in Table 3.

Table 3. MAD cleaner communication gateway and test PC specifications.

Device	Specifications	
Clium	Producer	Curaum Inc.
	Model Name	Clium
	MCU	ESP-WROOM-32D
	Bluetooth Version	Bluetooth v4.2
	Software	Clium v1.0
Test PC	Operating System	Windows 10 Home (64 bit)
	CPU	Intel® Core™ i7-8550U CPU 1.80 GHz
	RAM	16 GB
	SSD	256 GB
	NIC	Intel® Dual Band Wireless AC 8265 243.0 Mbps
	VGA	NVIDIA Geforce GTX 1050
	SW	Putty Release 0.68 [29], iperf-2.0.8b

The transmission speed results obtained from volunteer test patients are shown in Figure 8. The test environment was conducted according to the specifications mentioned in Section 3.2. All test procedures were approved by the Institutional Review Board (IRB) of Yonsei Severance Hospital (IRB approval number 2-2019-0060). Starting from a set time (time stamp = 0), the transmission speed was measured 26 times (n = 26) with a time interval of 2 s. All results were rounded up to the second decimal place. The results showed an average transmission speed of 91,870.19 bytes per second (standard deviation 136.3), with a population size of 25. The minimum value was 91,745, and the maximum value was 92,010, with a median of 91,869. The first quartile was 91,779.5, and the third quartile was 91,901, with the interquartile range of 121.5.

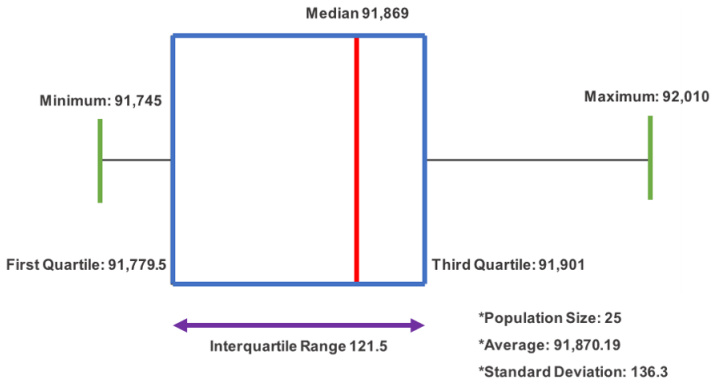

Figure 8. Transmission speed testing box and whisker plot results.

4.2. Wireless Connection Success Ratio Evaluation

A wireless Bluetooth connection success ratio evaluation was conducted to measure the seamless transmission of the proposed solution in a real-time usage scenario. The test scheme shown in Figure 9 was conducted under the conditions specified in Section 4.1. The test cycle was repeated 10 times (n = 10).

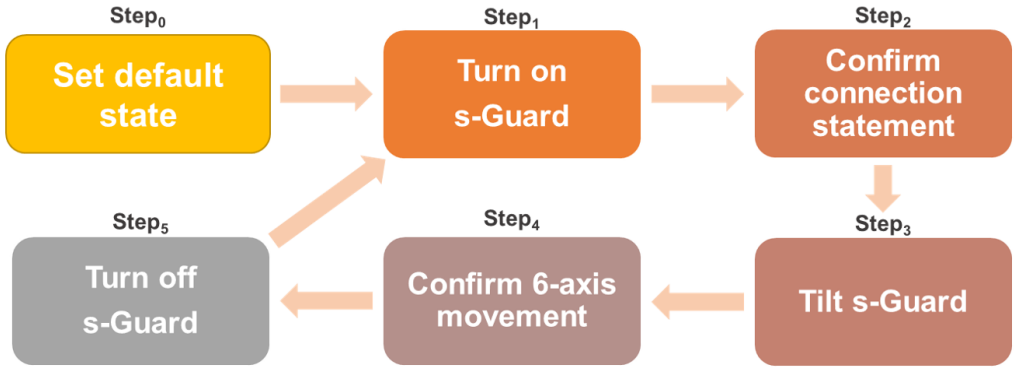

Figure 9. Connection success check test scenario cycle.

First, s-Guard was set to a default state ($Step_0$). It was switched from off to on ($Step_1$), which was the start of the first cycle. When pairing is complete, confirm the fixed connection statement "Now connected to the BLE Server" from the screen shown on the test computer ($Step_2$). Then, the tilt s-Guard is used to check the sensing connection ($Step_3$) and then check the screen that shows the six-axis values from the test computer again ($Step_4$). Here, six-axis values refer to combinations of values (2 × 3) calculated from the accelerometer (two-dimensional data) multiplied with gyroscope (x, y, z three-dimensional data). Finally, the s-Guard ($Step_5$) completes one cycle, and the next cycle begins. When the final $Step_5$ is completed, complete C_n and start another cycle. The final results indicated a success rate of 100%, as shown in Table 4.

Table 4. Connection success check test results.

Test Cycle	Six-Axis Value (Accelerometer and Gyroscope)						Connection Statement Confirmed	
							Positive	Negative
C_1	−96	152.4	914.7	−31,640.0	−1680.0	−12,670.0	O	
C_2	−194.3	141.2	913.2	2380.0	−210.0	0.0	O	
C_3	−184.3	149.9	980.3	2240.0	840.0	−280.0	O	
C_4	−194.9	114.6	982.2	2100.0	700.0	−1540.0	O	
C_5	−197.2	125.7	977.4	2170.0	210.0	3920.0	O	
C_6	−235.0	126.8	968.4	2800.0	−420.0	1470.0	O	
C_7	−218.2	144.8	971.0	350.0	−420.0	1470.0	O	
C_8	−307.4	247.1	926.6	2660.0	1540.0	−630.0	O	
C_9	−286.9	224.1	938.9	−2100.0	−280.0	3500.0	O	
C_{10}	−246.3	233.8	880.7	2170.0	−2170.0	420.0	O	
Total Success Rate							100%	

Accordingly, actual physiological signals of six-axis sensors (accelerometer and gyroscope) are shown in Figure 10. Figure 10a,b shows the accelerometer raw data and gyroscope data acquired by time. Each of the three colors of red, yellow, and blue in Figure 10a indicate x_1, y_2, and z_2 three-dimensional axes, respectively. On the other hand, each of the two colors of yellow and blue indicate x_2 and y_2 two-dimensional axes, respectively. Figure 10c shows the temperature data acquired by s-Guard. The blue line indicates raw data, the red line indicates linear average, and the green line indicates temperature

critical level threshold. Lastly, Figure 10d shows raw data acquired from the SpO_2 sensor from s-Guard. The green, red, and blue lines refer to SpO_2 raw data, heart rate, and infrared raw data, respectively.

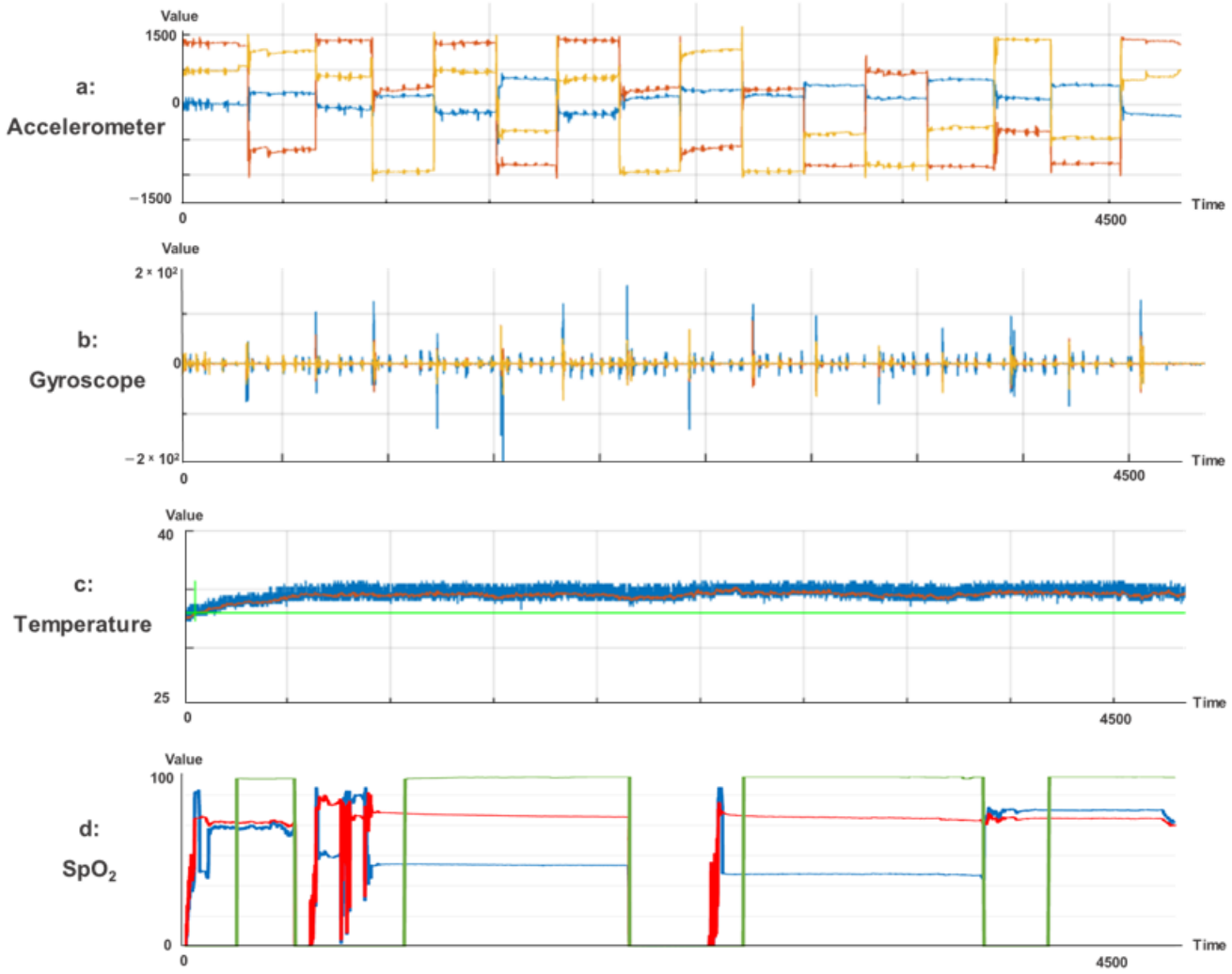

Figure 10. (**a**) Accelerometer signals; (**b**) gyroscope signals; (**c**) temperature signals; and (**d**) SpO_2 related signals.

4.3. Wireless Data Stream Error Ratio Evaluation

This section presents a wireless data stream error ratio evaluation. The target sample patient's aggregate sensor data signal was monitored up to a maximum length of 8 h. Data transmission status was measured at several set time intervals—first at 10 s, then at 100 s, 10 min, 1 h, 4 h, and finally, at 8 h. Eight hours was set because it is the most commonly known average suggested sleep time for adults.

According to theoretical calculations, the number of data transmission samples per second should be 250. This theoretical calculation was compared with the actual transmission sample calculation to assess the actual error rate. The measurement results are presented in Table 5. The results showed the highest error rate of 18.24% at 10 s elapsed time. However, the error rate greatly decreased as time passed. Eventually, the error rate decreased to a minimum of 0.1% when 8 h had fully elapsed.

Table 5. Wireless data stream error ratio evaluation results.

Elapsed Time	Transmitted Data (Samples)			Transmission Error Rate (%)
	Theoretical Calculation	Actual Calculation	Difference Error Samples	
10 s	2500	2044	456	18.24
100 s	25,000	24,284	716	2.86
10 min	150,000	149,178	822	0.55
1 h	900,000	898,510	1490	0.17
4 h	3,600,000	3,595,042	4958	0.14
8 h	7,200,000	7,192,854	7146	0.10

5. Discussion and Conclusions

This research proposed a multisensor embedded sleep quality health monitoring intraoral appliance device with innovative design and development features. Sleep quality could be improved by preventing bruxism and OSA via real-time monitoring and biofeedback.

s-Guard is fundamentally a wearable sensor. Therefore, assessing sensor stability in terms of wireless communication and seamless monitoring is most important. Necessarily, this can be assessed mainly by two categories: communication speed and communication errors.

The results revealed a wireless data transmission monitoring speed of 91,870.19 bytes per second, a connection success rate of 100%, and a minimum transmission error rate of 0.1%. Considering that previous research mentioned the problems regarding limited bandwidth in wireless health monitoring situations [30,31], this performance can be considered highly suitable.

Actual monitoring results showed successful sleep posture monitoring data calculated by the s-Guard algorithm based on sensed six-axis data. s-Guard was capable of monitoring a total of five sleep statuses: unidentified posture (null), prone position, supine position, leftward position, and rightward position. In addition, bruxism anomaly was also successfully detected by s-Guard, specifically monitored according to severity.

The solution proposed herein could contribute significantly to enhancing the sleep quality of modern lives, in which many people suffer from early age OSA and bruxism. OSA patients who have to use CPAP for intensive care may now use a much more compact and convenient method for treatment and management. In addition, this research opened the possibility of embedding sensors other than temperature, six-axis, and SpO_2. This is envisioned to be applied in various other fields of information communication technology (ICT) and IoT. In addition, s-Guard can be used in both medicine and everyday healthcare management.

A limitation of this research was that this solution was not suitable for short-term monitoring situations due to the high error rate in short-term sensing. Future research should investigate the reason for this and solve the issue of error rate so that this solution can also be used in short-term diagnosis situations.

Author Contributions: Conceptualization, S.-J.L. and I.-D.J.; methodology, E.-B.K.; software, I.-H.J.; validation, J.-Y.P. and J.-H.H.; formal analysis, S.-J.L.; investigation, E.-B.K. and J.-Y.P.; resources, J.-H.H., and T.-Y.J.; data curation, T.-Y.J.; writing—original draft preparation, S.-J.L., J.-H.H., and T.-Y.J.; writing—review and editing, I.-D.J. and T.-Y.J.; visualization, J.-Y.P.; supervision, T.-Y.J.; project administration, S.-J.L. and I.-D.J.; funding acquisition, S.-J.L., I.-D.J., and T.-Y.J. All authors have read and agreed to the published version of the manuscript.

Funding: This research was supported by a grant of the Korea Health Technology R&D Project through the Korea Health Industry Development Institute (KHIDI), funded the Ministry of Health & Welfare, Republic of Korea (grant number: HI19C1243), and the National Research Foundation of Korea (grant number: NRF-2020R1l1A1A01053726).

Institutional Review Board Statement: The study was conducted according to the guidelines of the Declaration of Helsinki, and approved by the Institutional Review Board (or Ethics Committee) of Yonsei Severance Hospital (IRB approval number 2-2019-0060).

Informed Consent Statement: Patient consent was waived due to nonidentifiable personal information included in this study.

Data Availability Statement: Not applicable.

Acknowledgments: All research results were certified by the Korea Testing Laboratory (KTL). The authors would like to thank the Electronics and Telecommunications Research Institute (ETRI) and Curaum Inc. for their experimental assistance.

Conflicts of Interest: The authors declare no conflict of interest.

References

1. Matsuda, M.; Ogawa, T.; Sitalaksmi, R.M.; Miyashita, M.; Ito, T.; Sasaki, K. Effect of mandibular position achieved using an oral appliance on genioglossus activity in healthy adults during sleep. *Head Face Med.* **2019**, *15*, 26. [CrossRef] [PubMed]
2. Braga, S.P.; Fiamengui, L.M.S.P.; da Silveira, V.R.S.; Chaves, H.V.; Furquim, B.D.; Cunha, C.O.; Repeke, C.E.P.; Conti, P.C.R. Insights for temporomandibular disorders management: From psychosocial factors to genetics—A case report. *Spec. Care Dent.* **2021**, *41*, 85–91. [CrossRef] [PubMed]
3. Madam, N.; Mosleh, W.; Punnanithinont, N.; Carmona-Rubio, A.; Said, Z.H.; Sharma, U.C. Pulmonary Arterial Enlargement is Associated with Acute Chest Pain in Patients without Obstructive Coronary Artery Disease. *Clin. Med. Insights Circ. Respir. Pulm. Med.* **2018**, *12*. [CrossRef] [PubMed]
4. Demonte, G.; Santangelo, D.; Roccia, F.; Gambardella, A.; Bono, F. Obstructive sleep apnea (OSA) in headache sufferers with Idiopathic intracranial Hypertension (IIH): A prospective study. *Cephalalgia* **2019**, *39*, 296–297.
5. Park, K.-M.; Kim, S.-Y.; Sung, D.; Kim, H.; Kim, B.-N.; Park, S.; Jung, K.-I.; Park, M.-H. The relationship between risk of obstructive sleep apnea and other sleep problems, depression, and anxiety in adolescents from a community sample. *Psychiatry Res.* **2019**, *280*. [CrossRef] [PubMed]
6. Philip, P.; Taillard, J.; Micoulaud-Franchi, J.-A. Sleep Restriction, Sleep Hygiene, and Driving Safety The Importance of Situational Sleepiness. *Sleep Med. Clin.* **2019**, *14*, 407–412. [CrossRef]
7. Johal, A.; Gill, G.; Ferman, A.; McLaughlin, K. The effect of mandibular advancement appliances on awake upper airway and masticatory muscle activity in patients with obstructive sleep apnoea. *Clin. Physiol. Funct. Imaging* **2007**, *27*, 47–53. [CrossRef]
8. Mezzanotte, W.S.; Tangel, D.J.; White, D.P. Influence of sleep onset on upper-airway muscle activity in apnea patients versus normal controls. *Am. J. Respir. Crit. Care Med.* **1996**, *153*, 1880–1887. [CrossRef]
9. Willman, M.; Igelström, H.; Martin, C.; Åsenlöf, P. Experiences with CPAP treatment in patients with obstructive sleep apnea syndrome and obesity. *Adv. Physiother.* **2012**, *14*, 166–174. [CrossRef]
10. Yetkin, O.; Kunter, E.; Gunen, H. CPAP compliance in patients with obstructive sleep apnea syndrome. *Sleep Breath.* **2008**, *12*, 365–367. [CrossRef]
11. Basyuni, S.; Barabas, M.; Quinnell, T. An update on mandibular advancement devices for the treatment of obstructive sleep apnoea hypopnoea syndrome. *J. Thorac. Dis.* **2018**, *10*, S48–S56. [CrossRef]
12. Chaves, C.M., Jr.; Dal-Fabbro, C.; Machado, M.; Bruin, V.; Bruin, P.; Gurgel, M.; Torgeiro, S.; Cevidanes, L.; Haddad, F.; Bittencourt, L. Use Of Mandibular Advancement Devices For Obstructive Sleep Apnoea Treatment in Adults. *Int. Arch. Med.* **2017**, *10*. [CrossRef]
13. Raja, J.M.; Elsakr, C.; Roman, S.; Cave, B.; Pour-Ghaz, I.; Nanda, A.; Maturana, M.; Khouzam, R.N. Apple Watch, Wearables, and Heart Rhythm: Where do we stand? *Ann. Transl. Med.* **2019**, *7*. [CrossRef]
14. Zhu, K.; Perrault, S.; Chen, T.; Cai, S.; Peiris, R.L. A sense of ice and fire: Exploring thermal feedback with multiple thermoelectric-cooling elements on a smart ring. *Int. J. Hum. Comput. Stud.* **2019**, *130*, 234–247. [CrossRef]
15. Jin, H.; Tao, X.; Dong, S.; Qin, Y.; Yu, L.; Luo, J.; Deen, M.J. Flexible surface acoustic wave respiration sensor for monitoring obstructive sleep apnea syndrome. *J. Micromech. Microeng.* **2017**, *27*, 115006. [CrossRef]
16. Rocher, J.; Parra, L.; Sendra, S.; Lloret, J. Smart System for Monitoring Apnea Episodes in Domestic Environments with Sound Sensor. In *International Conference on Advanced Intelligent Systems for Sustainable Development*; Springer: Berlin/Heidelberg, Germany, 2018; pp. 205–215.
17. Zhang, M.; Feng, H.; Luo, H.; Li, Z.; Zhang, X. Comfort and health evaluation of live mutton sheep during the transportation based on wearable multi-sensor system. *Comput. Electron. Agric.* **2020**, *176*, 105632. [CrossRef]
18. Nasiri, S.; Khosravani, M.R. Progress and challenges in fabrication of wearable sensors for health monitoring. *Sens. Actuators A Phys.* **2020**, *312*, 112105. [CrossRef]
19. Sekita, T.; Takeuchi, S.; Minakuchi, S. Measuring system for an attitude angle of a denture using an Inertial Measurement Unit. *J. Prosthodont. Res.* **2018**, *62*, 195–199. [CrossRef]
20. Jarchi, D.; Casson, A.J. Description of a Database Containing Wrist PPG Signals Recorded during Physical Exercise with Both Accelerometer and Gyroscope Measures of Motion. *Data* **2017**, *2*, 1. [CrossRef]

21. Shan, G.; Roh, B. Performance Model for Advanced Neighbor Discovery Process in Bluetooth Low Energy 5.0-Enabled Internet of Things Networks. *IEEE Trans. Ind. Electron.* **2020**, *67*, 10965–10974. [CrossRef]
22. Park, E.; Lee, M.-S.; Kim, H.-S.; Bahk, S. AdaptaBLE: Adaptive control of data rate, transmission power, and connection interval in bluetooth low energy. *Comput. Netw.* **2020**, *181*. [CrossRef]
23. Figueroa Lorenzo, S.; Anorga Benito, J.; Garcia Cardarelli, P.; Alberdi Garaia, J.; Arrizabalaga Juaristi, S. A Comprehensive Review of RFID and Bluetooth Security: Practical Analysis. *Technologies* **2019**, *7*, 15. [CrossRef]
24. Chia, J.; Yang, C. Thermal Management of QFN 48 Package Attached to Different Multi-Layers of Printed Circuit Board Designs. In Proceedings of the International Electronic Packaging Technical Conference and Exhibition, Maui, HI, USA, 6–11 July 2003; Volume 36908, pp. 57–61.
25. Atmel. *AT90USB82 Datasheet*, On-chip Analog, On-Chip Debug Interface, and Power-On Reset. ISP Flash and USB Controller AT90USB82, AT90USB162. Available online: https://www.digchip.com/datasheets/parts/datasheet/054/AT90USB162.php (accessed on 4 May 2021).
26. Maxim Integrated. *MAX30101 Datasheet: High-Sensitivity Pulse Oximeter and Heart-Rate Sensor for Wearable Health*; 2020. Available online: https://www.maximintegrated.com/en/products/interface/sensor-interface/MAX30101.html (accessed on 4 May 2021).
27. Anceschi, E.; Bonifazi, G.; De Donato, M.C.; Corradini, E.; Ursino, D.; Virgili, L. SaveMeNow. AI: A Machine Learning Based Wearable Device for Fall Detection in a Workplace. In *Enabling AI Applications in Data Science*; Springer: Berlin/Heidelberg, Germany, 2020; pp. 493–514.
28. Nordic Semiconductor. *nRF52840 Objective Product Specification v0.5.1*; 2017. Available online: https://infocenter.nordicsemi.com/pdf/nRF52840_OPS_v0.5.1.pdf (accessed on 6 July 2017).
29. Miele, P.; uwaisem, M.A.; Kim, D.-K. Comparative Assessment of Static Analysis Tools for Software Vulnerability. *JCP* **2018**, *13*, 1136–1144. [CrossRef]
30. Lee, S.-J.; Cho, G.-Y.; Lee, T.-R. N-WRETS: Near-Lossless Wireless Real-time Efficient Electroencephalogram Transmission Solution to Support Sleep Disorder Monitoring Platforms. *Telemed. e-Health* **2019**, *25*, 116–125. [CrossRef] [PubMed]
31. Cho, G.-Y.; Lee, G.-Y.; Lee, T.-R. Efficient Real-Time Lossless EMG Data Transmission to Monitor Pre-Term Delivery in a Medical Information System. *Appl. Sci.* **2017**, *7*, 366. [CrossRef]